STUDY OF TRANSIENT GROUND POTENTIAL RISE IN GAS-INSULATED SUBSTATIONS DURING FAULT CONDITIONS USING ELECTROMAGNETIC FIELD AND CIRCUIT THEORY APPROACHES

W. RUAN, F. P. DAWALIBI and J. MA
Safe Engineering Services & Technologies Ltd.
1544 Viel, Montreal, Quebec, Canada, H3M 1G4
Email: info@sestech.com Web site: http://www.sestech.com

Abstract: *This paper discusses in detail the computation of the transient ground potential rise (TGPR) in a 500 kV circuit breaker (CB) in a gas-insulated substation (GIS) during phase-to-ground faults. The faults are caused by a lightning strike on the phase conductor or a disconnect switch operation in the GIS. Models based both on electromagnetic fields and circuit theory have been used to predict the transient response. A reasonable agreement between the circuit model and field theory approaches is found in the presence of the grounding grid. The TGPR and transient electromagnetic fields near the CB exhibit an oscillation similar to that observed in the absence of the grounding grid [1]. The amplitude of the oscillation is reduced by about 50% due to lower surge ground impedances at the fault site. For the disconnect switching surge scenario, the transient GPR and electromagnetic fields oscillate initially at a higher frequency (around 1.8 MHz). The oscillation shows a very different waveform compared to the one for the lightning surge scenario. Two mitigation methods have been applied to the TGPR in the lightning surge scenario. It is found that the TGPR can be reduced significantly (as much as 40%) when the length of the ground strap of the circuit breaker is reduced by about a factor of two.*

Keywords: transient ground potential rise, gas insulated substation, electromagnetic field theory, circuit theory, computer modeling.

1. INTRODUCTION

Phase-to-ground faults in GIS usually take place between phase conductors and grounded tubular enclosures, due to dielectric breakdown of the SF_6 gas in the GIS. The breakdown can be caused by disconnect switch operations in the GIS [2] or lightning strikes to phase conductors in the GIS. These transients have been implicated in failures of protection and control circuits and in shocks to personnel.

The phase-to-ground faults which develop as a result of the lightning strike and the disconnect switch operation have been examined in our study. The results of the lightning surge scenario with no grid have been presented in Ref. [1]. The remaining computation results are presented here. For the completeness of this paper and convenience of the reader, the sections entitled "Description of The Problem" and "Computation Methods" in Ref. [1] have been included here with small modifications to suit this paper.

2. DESCRIPTION OF THE PROBLEM

Figure 1(a) shows a 500 kV SF6 circuit breaker and a substation grounding system. In this study, only the main conductors of the grounding system to which the breaker is connected have been modeled, as shown in the figure. To simplify the study, we have modeled only the faulted phase, since the transient behaviour is dominated by the faulted phase. Each phase of the circuit breaker is represented by a phase conductor, centered within a cylindrical wire mesh enclosure. A phase-to-ground fault is introduced by connecting the phase wire to the enclosure at the center of the enclosure (see Figure 1(a)). A resistive load (R) of 44 Ω is assumed to exist in the circuit prior to the transient fault occurrence.

The grounding system consists of a 20 × 25 m grid buried at a depth of 0.5 m and several 3.0 m long vertical ground rods which are driven to a depth of 3.5 m. The conductors of the grounding system are made of stranded copper wire, with a radius of 7 mm. The transmission line phase conductors are 1565 kcmil 36/7 ACSR conductors. For simplicity, the same type of conductor is also used for the phase conductors inside the tubular enclosures. A uniform soil with a 100 Ω-m resistivity, a relative permeability of 1 and relative permittivity of 1 is assumed.

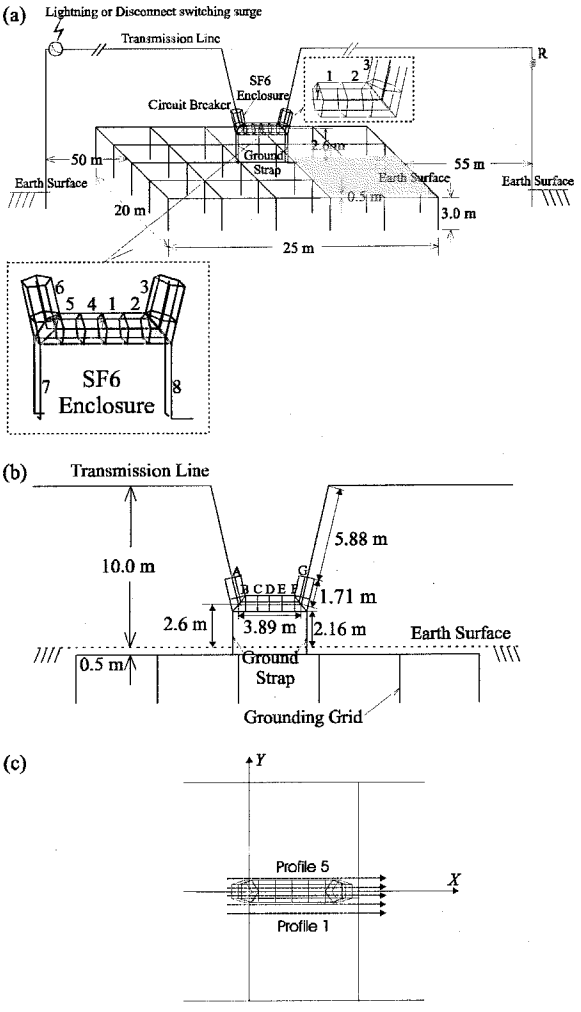

Figure 1. (a) A 500 kV circuit breaker and substation grounding system. (b) Side view of the transmission line and the circuit breaker. (c) Five observation point profiles.

In the field theory approach, a wire mesh is used to represent the tubular enclosure, as shown in Figure 1(a). Because we are interested in fault conditions at the circuit breaker, only five parallel (along the enclosure's axis) conductors are needed to represent the enclosure accurately (based on a previous study [3]). They are equally spaced around the circumference of the pipe and consist of aluminum conductors, with a diameter of 2 inches (5.08 cm). They represent a 2-inch thick aluminum pipe wall. The mean radius (average of inner and outer radius) of the pipe is $\overline{R} = 0.54$ m.

Figure 1(b) shows the dimensions of the circuit breaker. The transmission line is 10 m above the ground. The enclosure is subdivided into six sections. The letters A to G are used to label each section.

The ground potential rise (GPR) on the tubular enclosure as well as the scalar potentials and electromagnetic fields near the circuit breaker has been examined. The scalar potentials and electromagnetic fields have been computed at a number of observation points located on a horizontal plane, 1.5 m above the earth surface. As shown in Figure 1(c), the observation points are defined by 5 parallel profiles beneath the circuit breaker from $Y = -1$ to $Y = +1$ m, in 0.4 m steps. Each profile consists of 36 observation points starting at $X = -1.0$ m and spaced 0.2 m apart.

In the lightning surge scenario, the breakdown in the CB is assumed to occur as a result of a lightning strike on the transmission line, about 60 m away from the CB (see Figure 1(a)). The lightning surge is modeled as an ideal *current* source whose wave shape is a double exponential given by

$$I(t) = I_m\left[e^{-\alpha t} - e^{-\beta t}\right], \qquad (1)$$

where $I_m = 30$ kA, $\alpha = 1.4\times10^4$ sec^{-1} and $\beta = 6.0\times10^6$ sec^{-1} Figure 2 displays the waveform of the lightning surge current. The waveform of the lightning surge is characterized by a rise time of 1 μs and a half-value time of 50 μs.

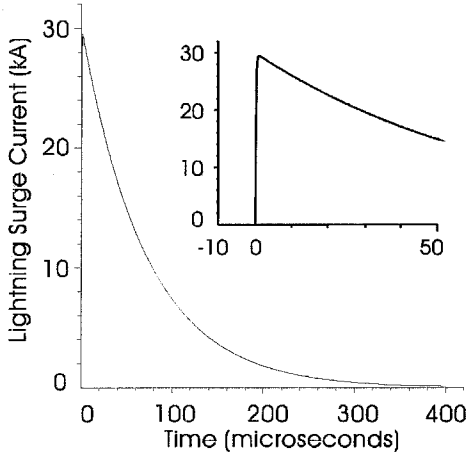

Figure 2. A double exponential lightning surge current.

In the switching surge scenario, the line-to-ground fault in the CB is assumed to be caused by a dielectric breakdown in a disconnect switching operation in the GIS which generates a surge voltage (60 m away from the CB) on the transmission line with a magnitude equal to the line-to-ground potential at the breakdown site. The 1.0 pu surge on the transmission line is represented by an ideal *voltage* source whose wave shape is again defined by a double exponential type

$$V(t) = V_m\left[e^{-\alpha t} - e^{-\beta t}\right], \qquad (2)$$

where $V_m = 1.0$, $\alpha = 2.31049\times10^5$ sec^{-1} and $\beta = 8.173503712\times10^9$ sec^{-1}. Figure 3 displays the waveform of the switching surge voltage. The waveform of the

switching surge is characterized by a rise time of 10 ns and a half-value time of 3 μs.

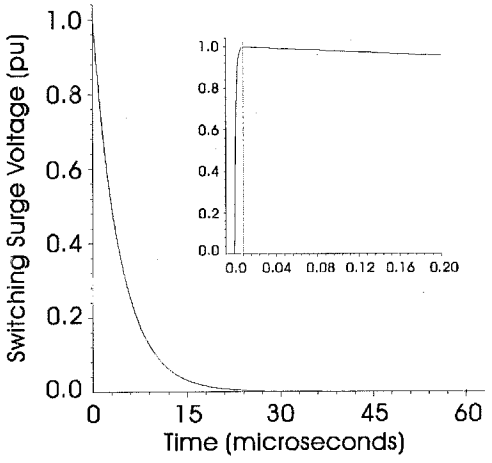

Figure 3. A double exponential switching surge voltage.

The frequency spectrums of the surge signals are obtained by taking the Fourier Transform of the time domain signals. The significant frequency components of the lightning surge are all below 7 MHz, while those related to the switching surge reach frequencies as high as 60 MHz.

3. COMPUTATION METHODS

To obtain the transient GPR and electromagnetic fields, a number of representative frequencies are selected from the frequency spectrum of the surge signal and then used to compute the frequency domain responses of the GPR and electromagnetic fields. The inverse Fourier transform is applied to the frequency domain responses to obtain the transient GPR and electromagnetic fields. The computation of the frequency domain responses is carried out using the circuit model and the field theory approach. The following describes in detail the computation methods.

3.1 Computation Methodology

By means of the Fourier Transform, the scalar potential and electromagnetic field in the time domain can be found by

$$V(t) = \frac{1}{2\pi}\int_{-\infty}^{+\infty} V(\omega)e^{i\omega t}d\omega = \frac{1}{2\pi}\int_{-\infty}^{+\infty} V_0(\omega)F(\omega)e^{i\omega t}d\omega \qquad (3)$$

$$E(t) = \frac{1}{2\pi}\int_{-\infty}^{+\infty} E(\omega)e^{i\omega t}d\omega = \frac{1}{2\pi}\int_{-\infty}^{+\infty} E_0(\omega)F(\omega)e^{i\omega t}d\omega \qquad (4)$$

$$H(t) = \frac{1}{2\pi}\int_{-\infty}^{+\infty} H(\omega)e^{i\omega t}d\omega = \frac{1}{2\pi}\int_{-\infty}^{+\infty} H_0(\omega)F(\omega)e^{i\omega t}d\omega \qquad (5)$$

where

$$F(\omega) = \int_{-\infty}^{+\infty} F(t)e^{-i\omega t}d\omega \qquad (6)$$

is the frequency spectrum of the surge signal (lightning current or surge voltage), as shown in Figures 2 and 3. $V_0(\omega)$, $E_0(\omega)$ and $H_0(\omega)$ are, respectively, the frequency spectrum of the scalar potential, electric field and magnetic field in the frequency domain.

$V_0(\omega)$, $E_0(\omega)$ and $H_0(\omega)$ are called the unmodulated system responses which are generated by applying a unit force energization to the conductor network. These responses define the characteristics of the conductor network in the frequency domain. They are independent of the input surge signal and, therefore provide valuable information about the frequency responses of the system being studied. The unmodulated system responses are modulated by the frequency spectrum of the surge signal $F(\omega)$ to obtain the so-called the modulated system response, which is used to obtain the time domain response via the inverse Fourier transform (Eqs. (3)-(5)). The computation of the unmodulated system response can be done using the circuit model and/or the field theory approach. The Multilines software subpackage of the CDEGS software [4] is used to compute the unmodulated system response using the circuit model approach. The unmodulated system response using the field theory approach is obtained using the Multifields software subpackage of the CDEGS software [4]. Both the forward and inverse Fourier transform are carried out by the FFTSES engineering module of Multifields.

3.2 Description of the Circuit Model Approach

A circuit model corresponding to the conductor network in Figure 1 is shown in Figure 4. The circuit is a two-terminal two-phase network corresponding to the phase conductor and the SF6 enclosure of the circuit breaker. The phase wire is energized by an electric source at the terminal site which simulates the lightning strike (using a current source) or the disconnect switch surge (using a voltage source). The phase-to-ground fault at the dielectric breakdown site is simulated by a short between the phase conductor and SF6 enclosure.

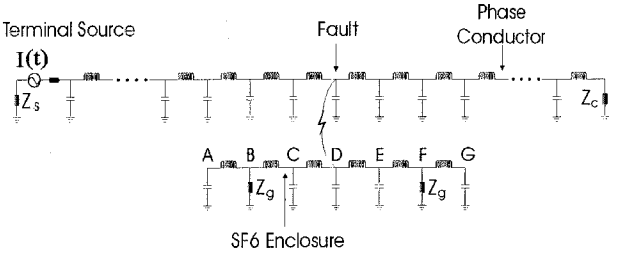

Figure 4. Circuit model representing the transmission line phase conductor and SF6 enclosure during a phase-to-ground fault.

The transmission line and SF6 enclosure in the circuit are divided into short sections. Note that Points A to G in Figure 4 correspond to Points A to G in Figure 1(b). In other words, the scalar potential at Point E in the circuit model corresponds to the GPR of Conductor Segment 1 in the field theory approach (see Figure 1(a)). For each section, the self impedance of each conductor, the inductive and capacitive mutual impedances between every pair of conductors and the shunt impedance of each conductor to ground are computed. These impedances are computed using the TRALIN module of the Multilines package. Interested readers may refer to [5,6] for information on line parameter computations. The impedance Z_g in the circuit represents the surge impedance of the ground straps (see Figure 1(a)) which includes the effects of the grounding grid. The impedances Z_s and Z_c of the phase conductor represent the equivalent neutral point ground impedances of the phase conductor at distances of 60 and 65 m respectively from the CB on each side of the breakdown site. These impedances were determined using the HIFREQ field theory module of the Multifields package.

The multiple-terminal multiple-phase network can be analyzed using the SPLITS module of Multilines, which is based on the double-elimination method described in [7] and on the generalization of this method to networks having arbitrary connections between conductors, including mutual capacitances [8]. Due to uncertainties related to circuit theory at frequencies above 10 MHz, the circuit model approach was used only for the lightning surge scenario. The TGPR in the switching surge scenario was computed using the field theory approach only.

3.2 Description of the Field Theory Approach

In the field theory approach, the metal enclosure is modeled as a collection of intersecting wires (meshed wires) and methods similar to those used in antenna theory are employed to compute the current distribution in the phase wire structure and the enclosure. The methods used to compute the current distribution and the electromagnetic fields generated by the energized conductor network are described in [9] and its references. The HIFREQ engineering module of the Multifields software package was used to perform the computations.

4. TGPR IN PRESENCE OF GROUNDING GRID DURING A LIGHTNING SURGE

4.1 Field Theory Approach

In this section, we will focus on examining the TGPR of Segments 1, 2 and 3 on the SF6 enclosure to compare the field theory approach with the circuit model approach. As shown in Figure 1, Segments 1, 2 and 3 correspond to Point E, F and G, respectively, in the circuit model (see Figure 4). The TGPR of Segments 7 and 8 on the ground strap will also be examined to see the influence of the grounding grid.

Figures 5 to 7 show the unmodulated scalar potentials, the modulated scalar potentials and the time domain transient ground potential rises for Segment 1, respectively. The spectrum again indicates that the lightning surge signal is dominated by its low frequency components. The TGPR initially oscillates at a resonance frequency of 1.05 MHz, then decays monotonically to zero. Note that the resonance frequency in the presence of the grounding grid is lower than it is without the grounding grid.

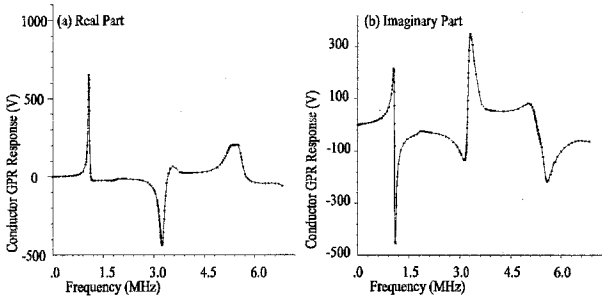

Figure 5. Real and imaginary parts of unmodulated scalar potential on Segment 1.

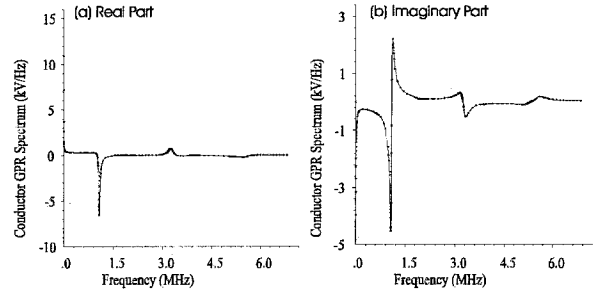

Figure 6. Real and imaginary parts of modulated scalar potential on Segment 1.

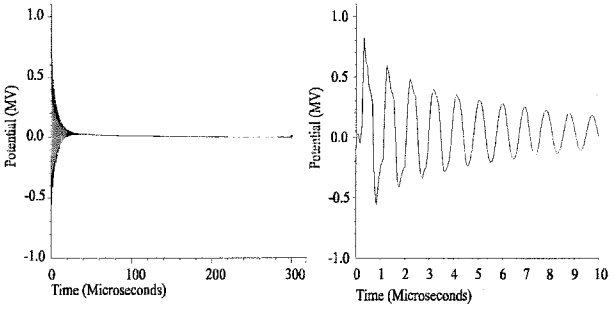

Figure 7. Transient ground potential rise on Segment 1.

Similar to the case without the grounding grid [1], the time domain TGPRs on Segments 2 and 3 are almost identical to the TGPR on Segment 1. However, the time

domain TGPR on Segments 6 and 7 is smaller than it is on Segment 1, due to the presence of the grounding grid (see Figure 8).

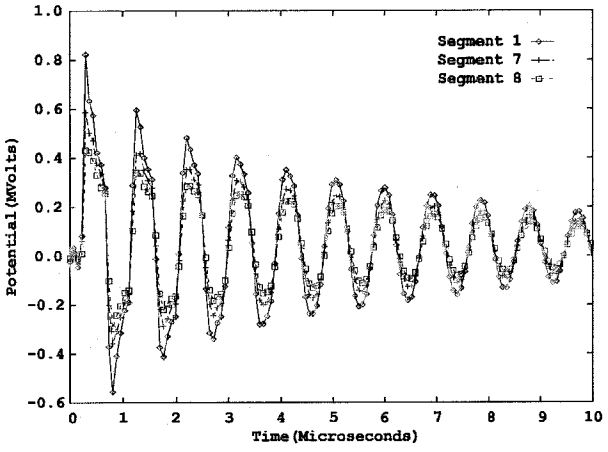

Figure 8. Comparison of TGPR on Segments 1, 7 and 8.

4.2 Comparison of Field Theory and Circuit Model Approaches

Figures 9 and 10 compare the unmodulated scalar potential and the TGPR produced by the two approaches. As shown in Figure 10, the TGPR on Segment 1 computed using the two approaches agrees reasonably well. The small difference is caused mainly by the modeling of the grounding grid. In the field theory approach, the grid is modeled exactly, whereas in the circuit model approach, the influence of the grid is approximated by the two surge impedances Z_g in the circuit shown in Figure 4 (note that Z_g was obtained using the field theory approach). The surge impedance Z_g is assumed to be twice that of the grounding grid impedance. Note that this approximation becomes invalid as the frequency increases to very high values. Reasonably good agreement is also observed for Segments 2 and 3 between the circuit model and the field theory approaches.

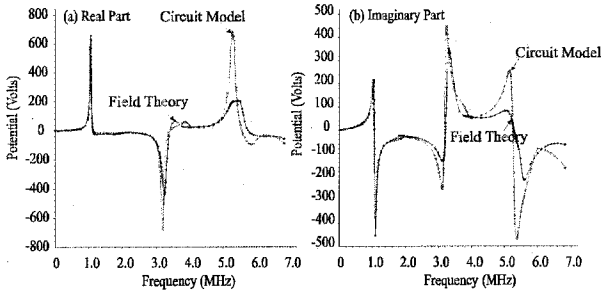

Figure 9. Comparison of unmodulated scalar potential computed using field theory and circuit model approaches for Segment 1 in presence of grounding grid.

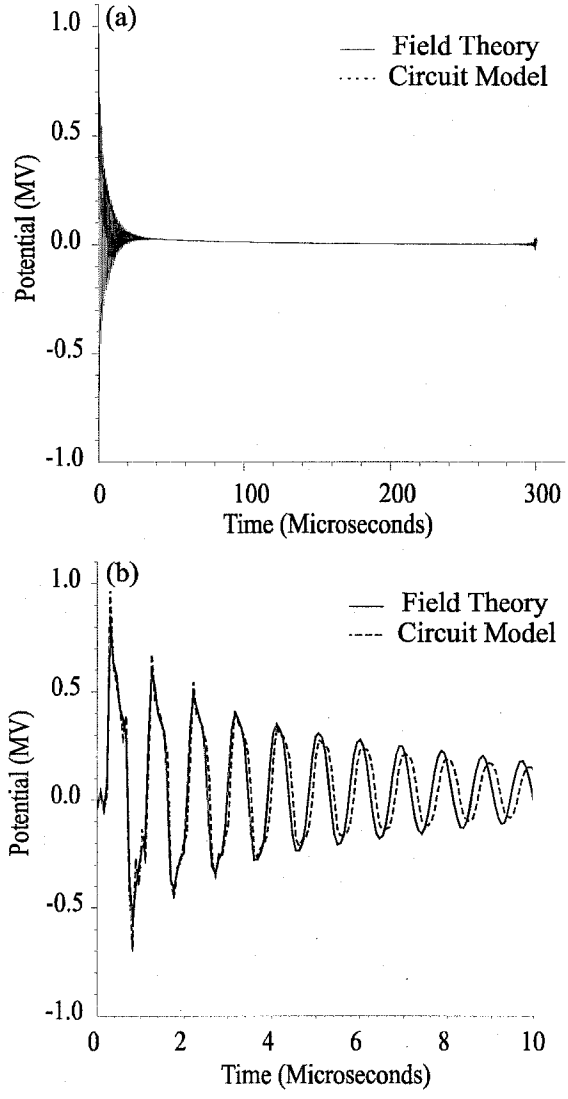

Figure 10. Comparison of TGPR computed using field theory and circuit model approaches for Segment 1 in presence of grounding grid.

5. TGPR IN PRESENCE OF GROUNDING GRID DURING A DISCONNECT SWITCHING SURGE

The transient ground potential rise due to a switching surge is computed using *only* the field theory approach. The circuit model approach can no longer be used since the switching surge signal contains the very high frequency components which exceed the range for which the software used for computing the transmission line parameters is valid. Using the field theory approach, the GPR and current distribution of conductor segments can be obtained. The electromagnetic fields near the circuit breaker are also obtained. Again, we will focus our attention on examining the TGPR near the fault site (Segments 1 to 8).

Figures 11 to 13 show the unmodulated scalar potential, the modulated scalar potential and the time domain transient ground potential rise, respectively, for Segment 1. The modulated scalar potential is obtained using the disconnect switch surge shown in Figure 3, with a peak magnitude of 1 MV. As shown in Figure 12, the dominant resonance frequency is around 1.8 MHz which is higher than the resonance frequency in the lightning surge scenario. The TGPR due to the switching surge also displays a very different waveform from the one in the lightning surge. In addition to the dominant resonance frequency of 1.8 MHz, Figure 13 shows that there exist some high frequency components in the TGPR for the first 2 μs.

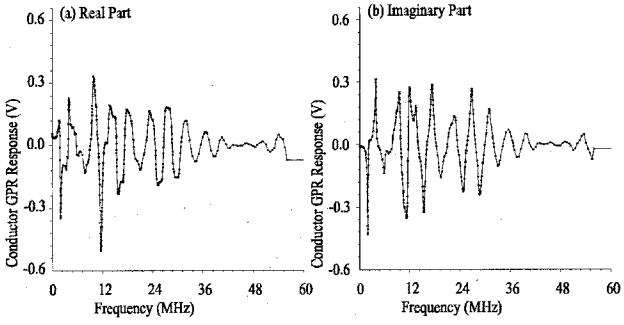

Figure 11. Real and imaginary parts of unmodulated scalar potential on Segment 1.

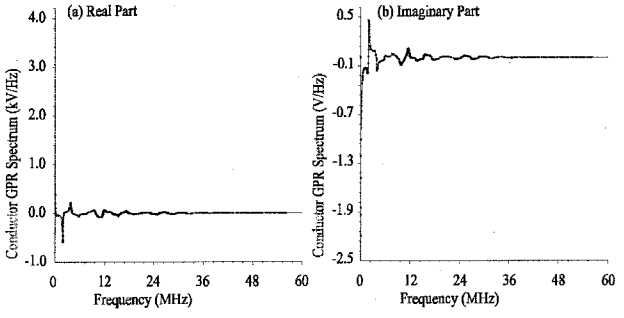

Figure 12. Real and imaginary parts of modulated scalar potential on Segment 1.

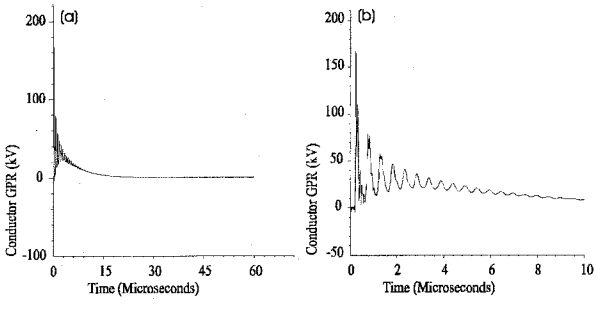

Figure 13. TGPR on segment 1. (a) full time window. (b) magnified time window.

Figure 14 compares the real and imaginary parts of the unmodulated scalar potential on Segments 1 to 3. The unmodulated system response in Figure 14 exhibits differences at higher frequencies (above 10 MHz). Such differences, again, do not lead to any significant changes in the time domain TGPR on Segments 2 and 3 (see Figure 15) due to the fact that the significant frequency components of the switching surge are also dominated by "low" frequency components.

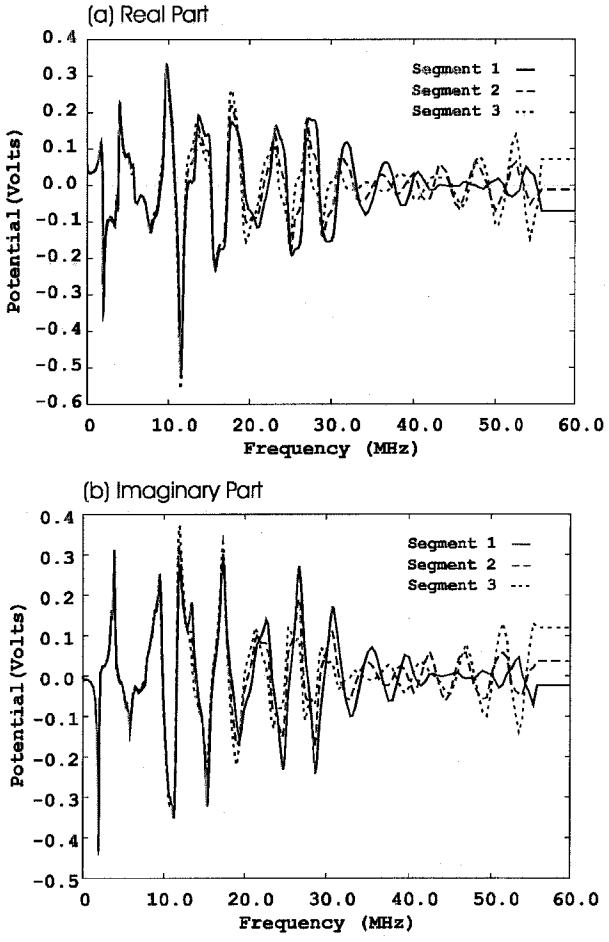

Figure 14. Comparison of unmodulated scalar potential on Segments 1, 2 and 3 during a switching surge

Figure 15 compares the TGPR on Segments 1 to 3 in the time domain. The magnitude of the TGPR on these segments is about the same. A time shift with respect to the TGPR on Segment 1 is observed for the TGPR on Segments 2 and 3. The time shift corresponds to the traveling time between the segments. Figure 16 compares the TGPR on segments on both sides of the fault. Figure 16 indicates that the TGPR on Segments 4 to 6 has higher values than that on Segment 1. Due to the symmetry of the problem, similar oscillations are observed for the TGPR on these segments.

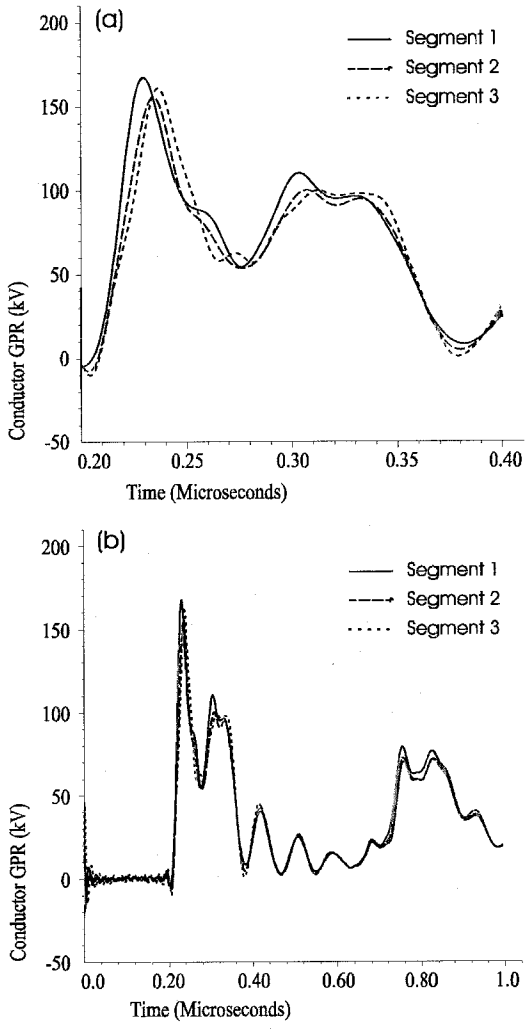

Figure 15. Comparison of TGPR on Segments 1 to 3 during a switching surge.

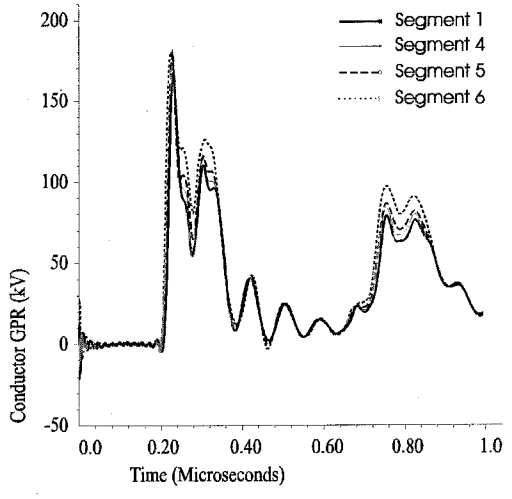

Figure 16. Comparison of TGPR on Segment 1 with TGPR on Segments 4, 5 and 6 on the CB during a switching surge.

Figure 17 compares the time domain TGPR on the ground strap (Segments 7 and 8) with the TGPR on Segment 1. As shown in Figure 17, the magnitude of the TGPR on the ground strap is smaller than that on the circuit breaker during the switching surge scenario.

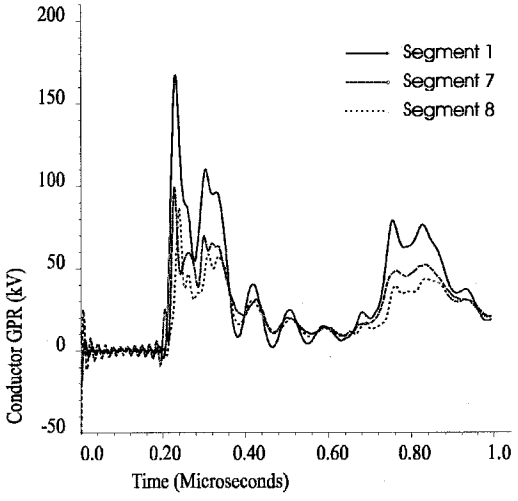

Figure 17. Comparison of TGPR on ground strap (Segments 7 and 8) with the TGPR on Segment 1.

6. MITIGATION OF THE TRANSIENT GROUND POTENTIAL RISE

In this section, the transient ground potential rise will be mitigated based on the following two techniques which were first introduced by Fujimoto *et al* [10]. The first method, which is described in Section 6.1, is to reduce the TGPR by changing the soil resistivity at the GIS. The second method, which is described in Section 6.2, is to reduce the TGPR by reducing the height of the ground strap of the circuit breaker. The mitigation effectiveness has been investigated using the circuit model approach for the lightning surge scenario only.

6.1. TGPR Influenced by Soil Resistivity

Using the circuit model approach, the TGPR on the circuit breaker at the fault site can be re-computed quickly for a soil resistivity of 20 Ω-m. The circuit model computation procedure requires only that the soil resistivity be changed from 100 Ω-m to 20 Ω-m. No other changes are required. The results are compared with the results corresponding to the 100 Ω-m soil which have been presented in Section 4.2. The computation is carried out in the presence of the grounding grid.

Figure 18 shows the TGPR on Segment 1 in Figure 1 for a soil resistivity of 20 Ω-m and 100 Ω-m. As can be seen in Figure 18, although the TGPR for a soil resistivity of 20 Ω-m resonates with a greater magnitude than that for

the 100 Ω-m soil, the TGPR for the 20 Ω-m soil decays more quickly than that for the 100 Ω-m soil. Similar behaviour is observed for the TGPR on Segments 2-6.

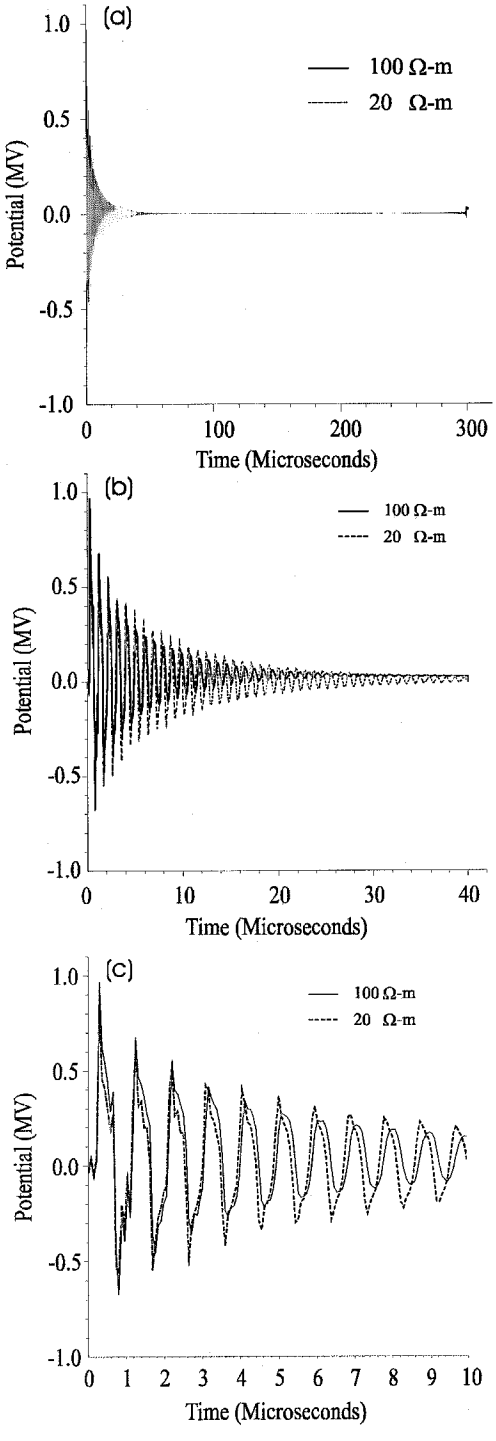

Figure 18. Computed TGPR at fault site (Segment 1 in Figure 1) using the circuit model and soil resistivities 100 Ohm-m and 20 Ohm-m: (a) full time window; (b) and (c) magnified time windows.

6.2 TGPR Influenced by Ground Strap

In this section, we present the TGPR computed for a short ground strap using the circuit model approach. The circuit breaker is lowered closer to the earth surface by reducing the ground strap length from 2.1631 m to 1 m. The TGPR on the circuit breaker at the fault site is computed and the results are compared with those corresponding to a 2.1631 m ground strap length as shown in Section 4.2. Again, the computation is carried out in the presence of the grounding grid.

Figure 19 shows the reduction of the TGPR on Segment 1 when the ground strap length is reduced by about a factor of two. As shown in Figure 19, the TGPR on the circuit breaker is reduced by as much as 40% when the ground strap length is decreased from 2.1631 m to 1 m. A similar reduction is also observed for the TGPR on Segments 2-6.

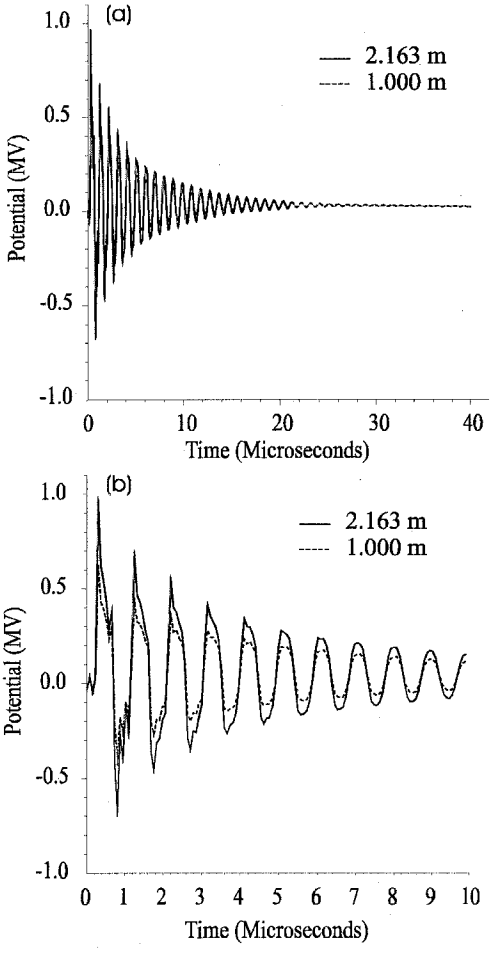

Figure 19. Computed TGPR at fault site (Segment 1 in Figure 1) using the circuit model, for the ground strap lengths of 2.1631 m and 1 m: (a) full time window; (b) magnified time window.

7. CONCLUSIONS

It is found that the TGPR computed using the circuit model and field theory approaches agrees well in the absence of the grounding grid. The TGPR and transient electromagnetic fields near the CB exhibit a monotonical decay preceded by a decaying oscillatory behaviour dominated by a resonance frequency of about 1.1 MHz.

A reasonable agreement between the circuit model and field theory approaches is also found in the presence of the grounding grid. The TGPR and transient electromagnetic fields near the CB also exhibit a monotonical decay preceded by a decaying oscillatory behaviour dominated by a lower resonance frequency of about 1.05 MHz. The TGPR values show an oscillation similar to that shown in Figure 8 in Ref. [1]. The amplitude of the oscillation is reduced by about 50% due to lower surge ground impedances at the fault site.

For the disconnect switching surge scenario, the transient GPR and electromagnetic fields oscillate initially at a higher frequency (around 1.8 MHz). The oscillation shows a very different waveform compared to the one for the lightning surge scenario.

In the lightning surge scenario, the TGPR can be reduced significantly (as much as 40%) when the length of the ground strap of the circuit breaker is reduced by about a factor of two. When the soil resistivity decreases from 100 Ω-m to 20 Ω-m, the TGPR oscillates with an increased amplitude, but decays towards zero more quickly. It appears that the TGPR can be mitigated more effectively by reducing the length of the ground strap.

8. ACKNOWLEDGMENTS

The authors wish to thank Safe Engineering Services & technologies ltd. for the financial support and facilities provided during this research effort. They also thank Mr. R. Southey for his help and constructive comments.

9. REFERENCES

[1] H. Lee, F. P. Dawalibi, J. Ma, W. Ruan and J. Kim "Comparison of Models Based On Electromagnetic Fields and Circuit Theory For The Computation of Transient Ground Potential Rise In Gas-Insulated Substations", *Proceedings of the International Conference on Electrical Engineering '97, Matsue, Japan*, 238-241, July, 1997.

[2] N. Fujimoto, E. P. Dick, S. A. Boggs, and G. L. Ford: "Transient Ground Potential Rise in Gas Insulated Substations - Experimental Studies", *IEEE Trans. On Power Apparatus and Systems*, **101**, 3603-3609, Oct. 1982.

[3] H. Lee, F. P. Dawalibi, W. Ruan and S. Fortin: "Performance of Gas-Insulated Substations and Associated Grounding Networks During Fault and Transient Conditions", *Proceedings of The 58th American Power Conference*, Chicago, 1591-1596, April 1996.

[4] F. P. Dawalibi and F. Donoso, "Integrated Analysis Software for Grounding, EMF, and EMI", *IEEE Computer Applications in Power*, Vol. 6, No. 2, pp. 19-24, 1993.

[5] J. R. Carson, "Wave Propagation in Overhead Wires with Ground Return", *Bell Syst. Tech. J.*, Vol. 5, pp. 539-554, 1926.

[6] M. Nakagama, et al., "Further Studies on Wave Propagation in Overhead Lines with Ground Return", *Proc. IEE*, Vol. 120, pp. 1521-1528, 1973.

[7] F. P. Dawalibi, *Transmission Line Grounding*, Vol. 1, Chapter 6, EPRI report EL-2699, Oct. 1982.

[8] J. Ma, "Analysis of Fault Current Distribution in a Power System Network", Research Report, Safe Engineering Services & technologies ltd., Montreal, Canada, Jan. 1993.

[9] S. Fortin, F. P. Dawalibi, J. Ma, and W. Ruan: "Effects of AC Power Line Configuration and Current Unbalance on Electromagnetic Fields", *Proceedings of The 57th American Power Conference*, Chicago, 170-175, April 1995.

[10] E. P. Dick, N. Fujimoto, G. L. Ford, and S. Harvey: "Transient Ground Potential Rise in Gas Insulated Substations - Problem Identification and Mitigation", *IEEE Trans. On Power Apparatus and Systems*, **101**, 3610-3619, Oct. 1982.

BIOGRAPHIES

Dr. Winston Ruan was born in Gansu, P. R. China in October 1964. He received the B.Sc. degree in physics from Lanzhou University, P. R. China in 1985. He received the Ph.D. degree in experimental physics in 1993, from the University of Manitoba, Winnipeg, Canada, where he worked from 1987 to 1992 on constructing a SQUID AC susceptometer/ magnetometer and studied magnetic phase transitions in reentrant magnetic alloys with quenched structural disorder. In 1993, he worked on Electrical Impedance Tomography using induced current methods, as a postdoctoral fellow in the Institute of Biomedical Engineering at Ecole Polytechnique, University of Montreal.

Since April 1994, he has been with the R&D Department of Safe Engineering Services & technologies ltd. His research interests include the computation of electromagnetic fields at various frequencies and transient phenomena.

Dr. Farid P. Dawalibi (M'72, SM'82) was born in Lebanon in November 1947. He received a Bachelor of Engineering degree from St. Joseph's University, affiliated with the University of Lyon, and the M.Sc. and

Ph.D. degrees from Ecole Polytechnique of the University of Montreal. From 1971 to 1976, he worked as a consulting engineer with the Shawinigan Engineering Company, in Montreal. He worked on numerous projects involving power system analysis and design, railway electrification studies and specialized computer software code development. In 1976, he joined Montel-Sprecher & Schuh, a manufacturer of high voltage equipment in Montreal, as Manager of Technical Services and was involved in power system design, equipment selection and testing for systems ranging from a few to several hundred kV.

In 1979, he founded Safe Engineering Services & Technologies, a company which specializes in soil effects on power networks. Since then he has been responsible for the engineering activities of the company including the development of computer software related to power system applications.

He is the author of more than one hundred papers on power system grounding, lightning, inductive interference and electromagnetic field analysis. He has written several research reports for CEA and EPRI.

Dr. Dawalibi is a corresponding member of various IEEE Committee Working Groups, and a senior member of the IEEE Power Engineering Society and the Canadian Society for Electrical Engineering. He is a registered Engineer in the Province of Quebec.

Dr. Jinxi Ma was born in Shandong, P.R. China in December 1956. He received the B.Sc. degree in radioelectronics from Shandong University, and the M.Sc. degree in electrical engineering from Beijing University of Aeronautics and Astronautics, in 1982 and 1984, respectively. He received the Ph.D. degree in electrical and computer engineering from the University of Manitoba, Winnipeg, Canada in 1991. From 1984 to 1986, he was a faculty member with the Dept. of Electrical Engineering, Beijing University of Aeronautics and Astronautics. He worked on projects involving design and analysis of reflector antennas and calculations of radar cross sections of aircraft.

Since September 1990, he has been with the R & D Dept. of Safe Engineering Services & Technologies in Montreal, where he is presently serving as manager of the Analytical R & D Department. His research interests are in transient electromagnetic scattering, EMI and EMC, and analysis of grounding systems in various soil structures.

Dr. Ma has authored and coauthored more than forty papers on transient electromagnetic scattering, analysis and design of reflector antennas, power system grounding, lightning and electromagnetic interference analysis. He is a corresponding member of the IEEE Substations Committee and is active on Working Groups D7 and D9.